Surface Science 612 (2013) 31–36

Contents lists available at SciVerse ScienceDirect

Surface Science

journal homepage: www.elsevier.com/locate/susc

Dim C_{60} fullerenes on Si(111) $\sqrt{3} \times \sqrt{3}$ – Ag surface

D.V. Gruznev [a,b], A.V. Matetskiy [a,b], L.V. Bondarenko [a,b], A.V. Zotov [a,b,c], A.A. Saranin [a,b,*], J.P. Chou [d], C.M. Wei [d], Y.L. Wang [d]

[a] Institute of Automation and Control Processes, 5 Radio Street, 690041 Vladivostok, Russia
[b] School of Natural Sciences, Far Eastern Federal University, 690950 Vladivostok, Russia
[c] Department of Electronics, Vladivostok State University of Economics and Service, 690600 Vladivostok, Russia
[d] Institute of Atomic and Molecular Sciences, Academia Sinica, P.O. Box 23-166 Taipei, Taiwan

ARTICLE INFO

Article history:
Received 11 January 2013
Accepted 15 February 2013
Available online 24 February 2013

Keywords:
Atom–solid interactions
Silicon
Fullerene
Surface diffusion
Scanning tunneling microscopy
Density functional calculations

ABSTRACT

Scanning tunneling microscopy (STM) observations of the close-packed C_{60} fullerene arrays on Si(111) $\sqrt{3} \times \sqrt{3}$ – Ag surface have revealed the presence of dim C_{60} molecules which constitute 9–12% of all fullerenes. The dim C_{60} fullerenes reside ~1.6 Å lower than the bright ("normal") C_{60}. While the bright C_{60} are in continuous rotation, the dim C_{60} are fixed in one of the single orientations, indicating a more tight bonding to the surface. At room temperature (RT), the dynamic switching from bright to dim C_{60} and vice versa has been detected. Switching slows down with decreasing temperature and becomes completely frozen at 110 K, which implies that the switching is a thermally driven process. RT deposition of ~0.1 monolayer of Ag onto C_{60} array eliminates completely the dim C_{60} molecules. Experimental results can be understood if one assumes that formation of the dim C_{60} is associated with disintegration of Ag trimer on Si(111) $\sqrt{3} \times \sqrt{3}$ – Ag surface under a given C_{60} fullerene.

1. Introduction

C_{60} monolayers on crystalline surfaces have attracted a considerable interest due to their rich structural and electronic properties, which make them a promising material for molecular electronics. Interaction between C_{60} and substrate surface differs for different substrates and affects greatly electronic properties of the grown C_{60} layers. Within the same molecular layer, the fullerenes with the different bonding configurations can exhibit different properties. A vivid example is a scanning tunneling microscopy (STM) observation of the fullerenes having different apparent heights, so-called "bright" and "dim" C_{60} molecules [1,2]. The commonly accepted explanation for metal surfaces is that the bright C_{60} fullerenes reside atop the surface, hence having a weak bonding configuration, while the dim C_{60} fullerenes are characterized by a strong bonding configuration with the molecules occupying nanopits (vacancies). The size of a pit depends on the substrate material [3] (e.g., a single-atom vacancy pit for C_{60} on Ag(111) [4] or Pt(111) [5] and a seven-atom vacancy for C_{60} on Cu(111) [6] or Au(111) [7]). Pit formation enhances C_{60}-substrate bonding energy and facilitates charge transfer from the surface to C_{60} by adopting more C_{60}-metal bonds.

Compared to pure metal surfaces, much less is known about C_{60} interaction with metal/silicon surface phases, i.e. surface reconstructions induced by adsorption of metal monolayers or submonolayers onto Si crystalline substrates [8]. The most researches in this field have been devoted to adsorption of C_{60} onto Si(111) $\sqrt{3} \times \sqrt{3}$ – Ag surface [9–15] due its high perfection and chemical inertness. The other metal-terminated Si surfaces hosting C_{60} molecules under investigation include Si(111) $\sqrt{3} \times \sqrt{3}$ – B [16], Si(111)1×1-Pb [17], Si(111) $\sqrt{3} \times \sqrt{3}$ – In [18], Si(111)2×2-In and Si(111) $\sqrt{7} \times \sqrt{3}$ – In [19], Si(111) 4×1-In [20], and pure and In-modified Si(111) $\sqrt{3} \times \sqrt{3}$ – Au [21]. Adsorption behavior of C_{60} on metal-terminated Si surfaces resembles in some aspects that on pure metal surfaces, but similarity is not complete. For example, C_{60} molecules adsorbed onto Si(111)2×2-In, Si(111) $\sqrt{7} \times \sqrt{3}$ – In and Si(111)4×1-In surfaces displace In atoms from beneath C_{60} to the surrounding surface area [19,20], which is similar to vacancy pit formation on metal surfaces. However, only for C_{60} on Si(111)4×1-In indium displacement definitely leads to occupation of a strongly bonded adsorption state by C_{60} having dim STM appearance [20]. It is worth noting that the plausible driving force for In displacement is a tendency of C_{60} to change relatively modest bonding with In atoms to a more stronger bond with Si(111) substrate. In the case of Si(111) $\sqrt{3} \times \sqrt{3}$ – Ag [11] and Si(111) $\sqrt{3} \times \sqrt{3}$ – Au surfaces [21], specific dim–bright C_{60} patterns develop in the molecular layers, though the underlying surface reconstructions seem to preserve their structure undisturbed. In particular, the dark features are seen within the C_{60} arrays on Si(111) $\sqrt{3} \times \sqrt{3}$ – Ag which were interpreted

* Corresponding author at: Institute of Automation and Control Processes, 5 Radio Street, 690041 Vladivostok, Russia. Tel.: +7 4232310426; fax: +7 4232310452.
E-mail address: saranin@iacp.dvo.ru (A.A. Saranin).

0039-6028/$ – see front matter © 2013 Elsevier B.V. All rights reserved.
http://dx.doi.org/10.1016/j.susc.2013.02.007

as missing-molecule defects generated to release of strain energy at the molecular layer/substrate interface [11].

In the present study, we have reconsidered the "missing-molecule defects" in C_{60} arrays on Si(111) $\sqrt{3}\times\sqrt{3}-Ag$ surface and have found that they are actually the dim C_{60} molecules which are in a more tight bonding configuration and reside ~1.6 Å lower than the other C_{60} molecules. At room temperature, dynamical bright-to-dim C_{60} switching and vice versa takes place. Switching has been found to be a thermally driven process: it slows down with decreasing temperature and becomes completely frozen at 110 K. The density of dim C_{60} decreases with RT Ag dosing of the C_{60} array and they are completely eliminated after depositing ~0.1 ML of Ag. The plausible mechanism of dim C_{60} formation is associated with the disintegration of Ag trimer on Si(111) $\sqrt{3}\times\sqrt{3}-Ag$ surface under a given C_{60} molecule.

2. Experimental

Our experiments were performed with an Omicron STM operating in an ultrahigh vacuum (~7.0×10^{-11} Torr). Atomically-clean Si(111) 7×7 surfaces were prepared in situ by flashing to 1280 °C after the samples were first outgassed at 600 °C for several hours. Silver was deposited from an Ag-wrapped tungsten filament and C_{60} fullerenes from a resistively heated Mo crucible. Si(111) $\sqrt{3}\times\sqrt{3}-Ag$ surface was prepared by depositing 1 monolayer of Ag onto the Si(111)7×7 surface kept at 500 °C. The main defects at the prepared surface were the domain walls, while the density of point defects at the $\sqrt{3}\times\sqrt{3}-Ag$ domains was negligible (~0.001 ML). For STM observations, electrochemically etched tungsten tips cleaned by in situ heating were employed. All STM images shown in the paper were acquired in the constant-current mode at room temperature.

3. Results and discussion

Fig. 1 shows a typical STM image of C_{60} monolayer grown on Si(111) $\sqrt{3}\times\sqrt{3}-Ag$ surface at room temperature. In agreement with the previous STM observations [12], one can see that adsorbed C_{60} molecules form two types of close-packed molecular arrays on this surface. Tsuchie et al. [12] defined them as $\sqrt{21}\times\sqrt{21}-R\pm10.9°$ and $3\sqrt{3}\times3\sqrt{3}-R30°$. In our notation (which seems to us more accurate), these would be 19.1°-rotated and 30°-rotated arrays, respectively. Note that the rotation angle is that which C_{60} row makes with the main crystallographic direction on Si(111) surface, $[\bar{1}10]$. One can see that the dark features interpreted as "missing-molecule defects" by Nakayama et al. [11] are present in arrays of both types. Fraction of dark features is somewhat greater in the 30°-rotated arrays as compared to the 19.1°-rotated arrays (~0.12 versus ~0.09). Another apparent difference is the different arrangements of dark features. In the 19.1°-rotated, they form relatively long meandering chains or compact arrays without any long-range order, while in the 30°-rotated domains the short chains are arranged in a long-range quasi-periodic structure.

The results of high-resolution dual-polarity STM observations (see Fig. 2a) unambiguously demonstrate that dim C_{60} fullerenes are not missing-molecule defects, but C_{60} molecules in another bonding state. While the bright ("normal") C_{60} are plausibly in continuous rotation (producing a single round protrusion in STM images in both polarities), the fine intermolecular structure of dim C_{60} resolved in the filled-state STM images (as in the lower part of Fig. 2a) indicates that they are fixed in one of the several types of orientations (e.g., resulting in characteristic "three-lobe" and "striped" STM appearance). Fixation of the dark fullerenes in given orientations is a sign of their enhanced bonding to the substrate, as compared to that of the freely rotating bright C_{60}.

Fig. 3 demonstrates how the apparent height difference between bright and dim C_{60} depends on the applied sample bias voltage. One can see that the height difference is rather large (being ~1.6 ± 0.3 Å) and of the same sign at both polarities. Thus, one can conclude that it has mainly a topographical origin, i.e. the dim C_{60} molecules reside lower than the bright C_{60}. This seems quite natural for the more strong bonding state. However, one can notice a certain variation between the apparent height difference in filled and empty states. In particular, the difference is enhanced at positive sample bias (which is similar to the observations on C_{60}/Au(111) [1]). This is plausibly due to the electronic effects (e.g., due to difference in charge transfer to C_{60} occupying different bonding states).

By comparing consecutive STM images acquired at RT we have found that selected C_{60} molecules switch from bright-to-dim or vice versa. The switching takes place in a similar way both in the 19.1°-rotated and 30°-rotated C_{60} arrays. As an example, Fig. 4 presents the results for the 19.1°-rotated array. Fig. 4a–d show four successive STM images acquired from the same area of the C_{60} array with 20 s separation per scan (for a whole STM video see [22]). Fig. 4e–g shows subtractions of consecutive images, where white and dark spots correspond to the bright-to-dim and dim-to-bright switching events, respectively. One

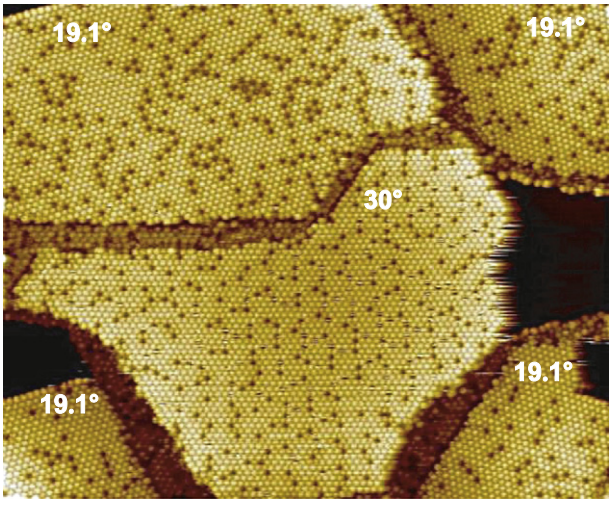

Fig. 1. 1000×820 Å^2 empty-state (+2.0 V) STM image of Si(111) $\sqrt{3}\times\sqrt{3}-Ag$ surface with small inclusions of 6×1-Ag phase after RT deposition of about one monolayer of C_{60} fullerenes. Two types of C_{60} arrays, 19.1°-rotated and 30°-rotated ones, are indicated.

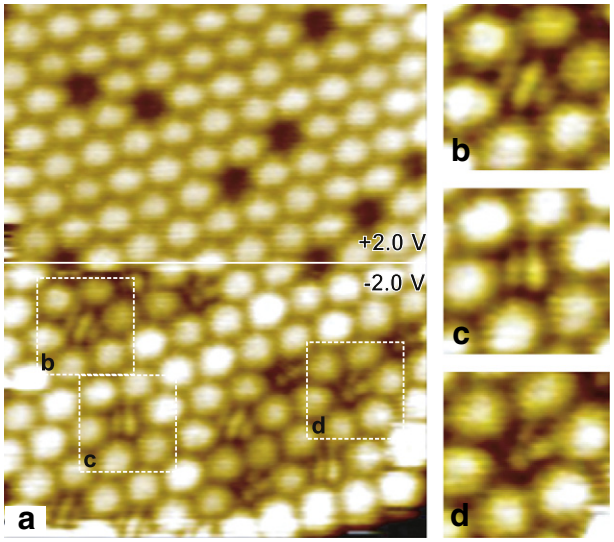

Fig. 2. (a) 115×160 Å^2 dual-polarity (±2.0 V) STM image of C_{60} array on Si(111) $\sqrt{3}\times\sqrt{3}-Ag$ surface. The dim C_{60} are seen as depressions in the empty-state image (upper panel), but their intermolecular structure can be clearly resolved in the filled-state image (lower panel). The typical intermolecular structures include (b) triple-striped, (c) double-striped, and (d) three-lobe ones.

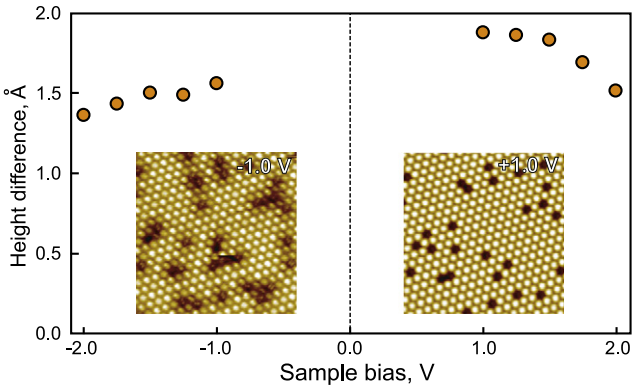

Fig. 3. Apparent height difference between bright ("normal") and dim C_{60} as a function of sample bias voltage. The insets show STM appearance of C_{60} array at −1.0 and +1.0 V. Acquisition of the STM images at bias voltages from −1.0 V to +1.0 V was hampered due to the presence of the energy gap between the HOMO and LUMO bands of the C_{60} layer.

can see that some of the dim C_{60} "jump" to the nearest lattice sites in the array (which events manifest themselves as pairs of white and dark spots), but many of them disappear and appear quite randomly. The variable-temperature observations have revealed that switching slows down with decreasing temperature and becomes completely frozen at 110 K [22]. This result implies that the switching is a thermally driven process.

Some details of the switching have been visualized in the experiment when an STM tip is placed above a given C_{60} and the tunneling current is monitored during a certain period of time. The typical plot of current versus time is shown in Fig. 5. Abrupt drop in the tunneling current highlights the bright-to-dim switching event, the low current plateau corresponds to the dim C_{60} state of the molecule and abrupt current increase indicates returning of the molecule to the bright (normal) C_{60} state. One can notice an essential difference between the two adsorption states. In the dim C_{60} state, the current value is stable, hence the molecule is tightly fixed in its site. In the bright C_{60} state, the current is fluctuating quasi-periodically, hence the molecule plausibly changes its vertical location.

Remarkable possibility for tuning the density of dim C_{60} has been disclosed in the experiment with RT dosing of the C_{60} arrays on Si(111) $\sqrt{3}\times\sqrt{3}$ – Ag with additional Ag. The results of this experiment are summarized in Fig. 6. One can see that after Ag depositions no Ag-associated features appear at the surface of the C_{60} layer, which implies that Ag atoms penetrate through molecular layer to the buried layer–substrate interface in agreement with the previously reported results [23]. However, these depositions appear to affect dramatically the density of dim C_{60} molecules which decreases with Ag dosing in a similar manner for both types of arrays. After depositing ~0.1 ML of Ag, no dim C_{60} are left in the arrays. In particular, this allows us to visualize the Moiré pattern in the 30°-rotated C_{60} arrays, which are otherwise masked by the presence of dim C_{60} molecules. In both polarities, the Moiré pattern has a honeycomb-like appearance with darker molecules forming hexagons and brighter molecules surrounding them. The periodicity of the Moiré pattern appears to be about $\sqrt{19}\times\sqrt{19}$. Note that the same periodicity has been found for the Moiré pattern in 0°-rotated C_{60} arrays on In-modified Si(111) $\sqrt{3}\times\sqrt{3}$ – Au surface, though the pattern there has quite a different appearance (the bright C_{60} residing atop Au trimers arranged in the $\sqrt{19}\times\sqrt{19}$ lattice [21]).

Unusual effect of Ag dosing on dim C_{60} density is believed to provide the most valuable hint for understanding origin of the dim C_{60} molecules. Thus, let us consider now how added Ag could affect the properties of the buried layer–substrate interface. The first guess is certain electronic effects since adsorption of additional Ag atoms onto Si(111) $\sqrt{3}\times\sqrt{3}$ – Ag is known to produce significant doping of surface-state band [24–26]. However, this is a specific feature not

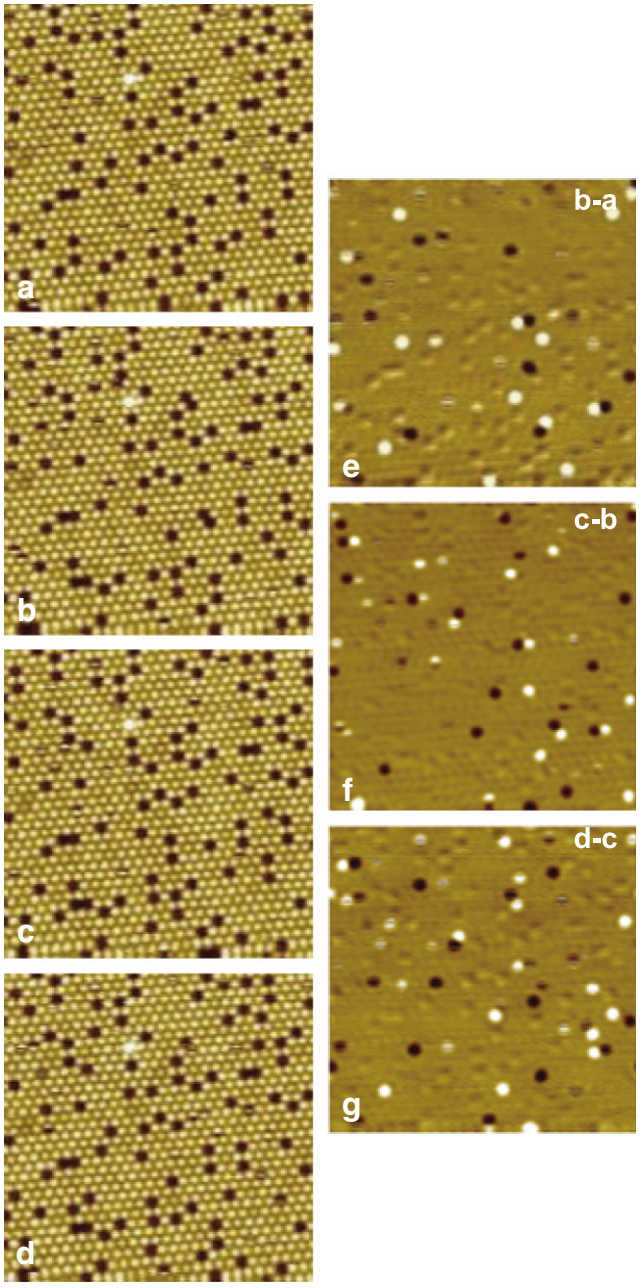

Fig. 4. (a)–(d) A series of four consecutive STM images of the same C_{60} array area (300×300 Å^2) acquired at RT. Selected C_{60} molecules are seen to switch from bright-to-dim and vice versa. (e)–(g) Subtractions of consecutive images, where white and dark spots correspond to the bright-to-dim and dim-to-bright switching events, respectively.

only of Ag but also is a common trait of alkali metals (e.g., Na [27–30]) which produce a similar electronic effect. Thus, one could expect that deposited Na would affect the dim C_{60} fraction in a same way as additional Ag. To check this possibility, we conducted an experiment with RT Na deposition onto C_{60} layer on Si(111) $\sqrt{3}\times\sqrt{3}$ – Ag which result is presented in Fig. 7. One can see that in contrast to Ag the adsorbed Na does not eliminate dim C_{60} fullerenes. Decrease, if any, in their density does not exceed 20%. Thus, one can conclude that electronic effects could hardly play a decisive role in the observed phenomenon.

In addition, we would like to note that the C_{60} molecule is known to act typically as an acceptor-type adsorbate on most surfaces, including Si(111) $\sqrt{3}\times\sqrt{3}$ – Ag [15,23]. Thus, electrons which would be otherwise donated from metal adsorbates, Ag or Na, to the surface state band might become trapped by the C_{60} molecules. Thus, possible electronic

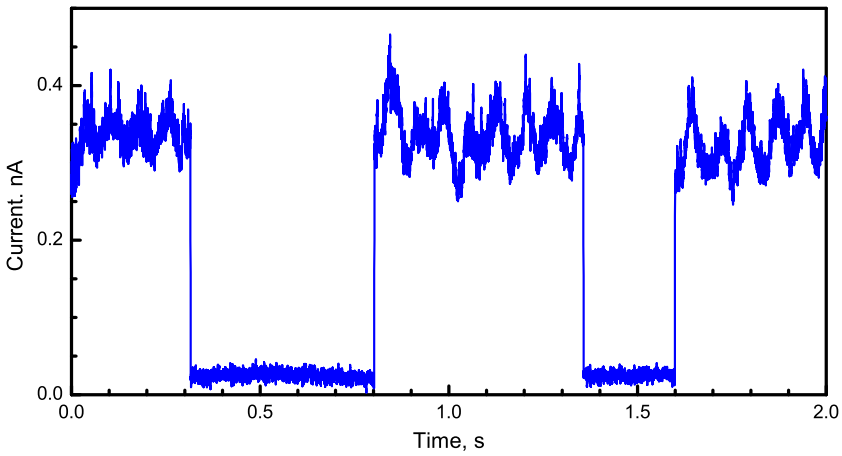

Fig. 5. Tunneling current between STM tip and C_{60} molecule as a function of time. The low-current values correspond to the fullerene in the dim C_{60} state, the noisy high-current value to the bright (normal) C_{60} state.

effects induced by metal adsorbates might be suppressed by the fullerenes. This consideration can be treated as an additional argument against the decisive role of electronic effects in elimination of the dim C_{60} fullerenes.

In other words, the appearance of dim C_{60} has plausibly an atomic origin. We would like to remind that dim C_{60} molecules on metal surfaces have been proved to be associated with pits formed at the surface under the fullerenes. In case of C_{60} on Au(111), these are seven-atom vacancies [7]. Dynamical switching from bright-to-dim C_{60} and vice versa observed in this system at RT [1] implies that seven-atom vacancy can appear, heal over and reappear again under given C_{60}. Similar process has recently been characterized quantitatively for a

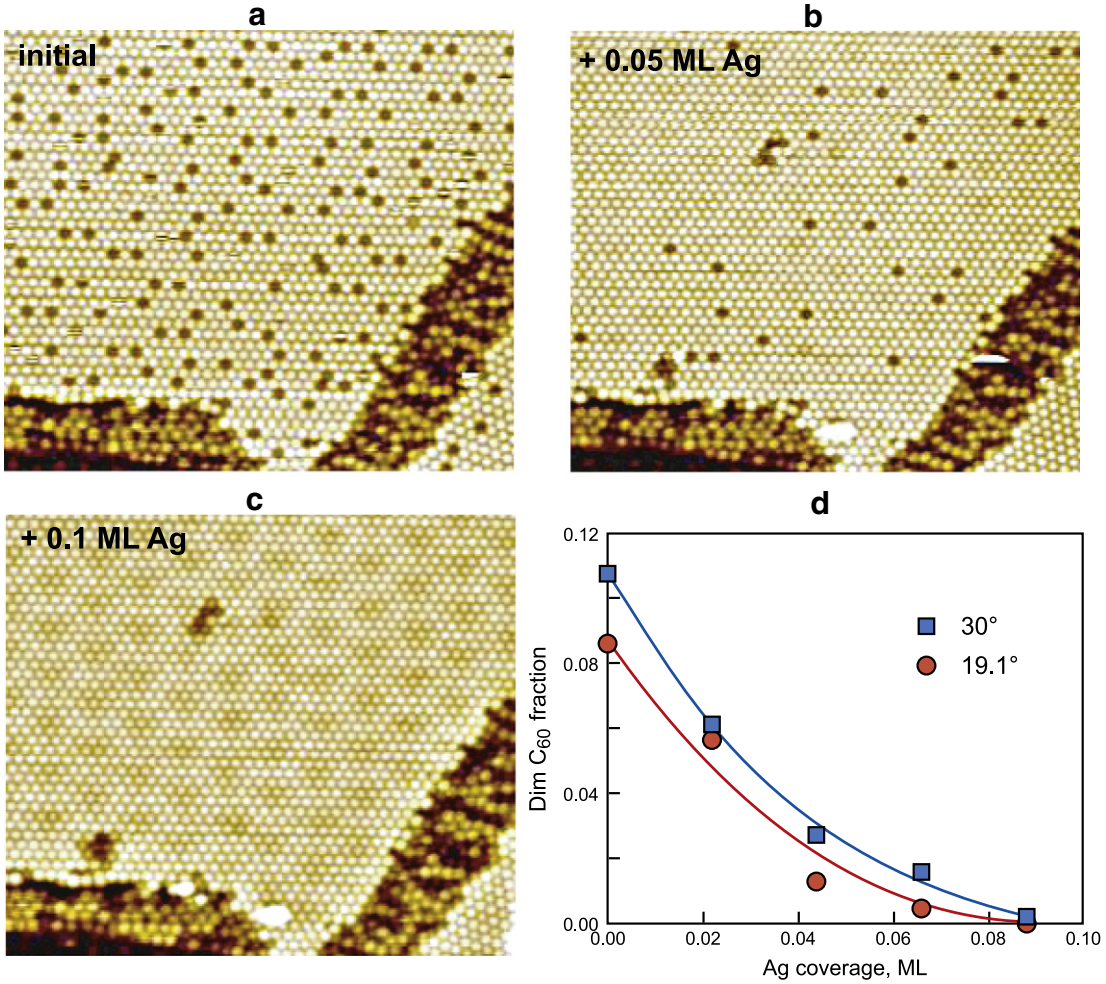

Fig. 6. Effect of RT deposition of additional Ag on the density of dim C_{60}. (a) 500×500 Å^2 empty-state (+2.0 V) STM image of the as prepared C_{60} array on Si(111) $\sqrt{3}\times\sqrt{3}$ – Ag. The same array after RT deposition of (b) 0.05 and (c) 0.10 ML of Ag. A plot of dim C_{60} fraction as a function of Ag dose for the 30°-rotated (blue squares) and 19.1°-rotated (red circles) C_{60} arrays.

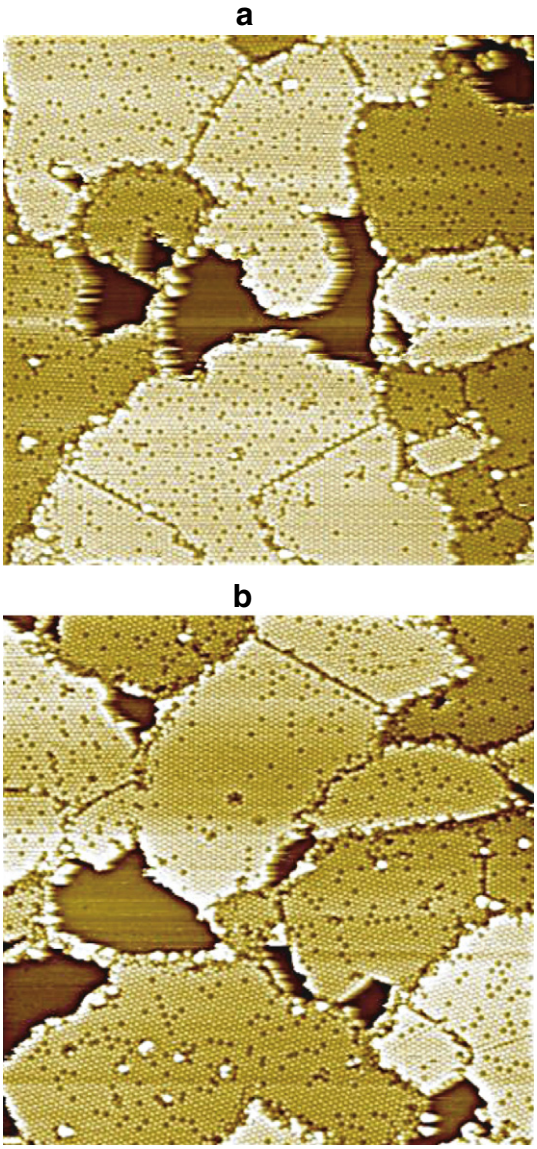

Fig. 7. 1000×1000 Å^2 empty-state (+1.8 V) STM images of the C_{60} layer on Si(111) $\sqrt{3}\times\sqrt{3}$ – Ag (a) before and (b) after RT deposition of Na. Images are taken from different surface areas.

dynamic equilibrium of C_{60} molecules on Ag(111) [2]. Such a behavior reflects a flexibility of the metal surfaces. Metal-induced silicon reconstructions are typically more solid. However, this concerns mainly a Si frame, while metal overlayers demonstrate a much greater degree of flexibility (e.g., as shown for Ag/Si(100) [31]). The Si(111) $\sqrt{3}\times\sqrt{3}$ – Ag surface is known to be built of Ag and Si trimers of which the Ag trimers are believed to be "the weakest link". In particular, agility of Ag atoms shows up in the order–disorder transition occurring in the Ag-trimer structure at ~150 K [32–34]. Thus, it is natural to suppose that Ag trimers can disintegrate into individual Ag adatoms and the density of disintegrated Ag trimers is controlled by the density of 2D gas of Ag adatoms present at the surface. The higher the density of adatoms (say, as a result of additional Ag deposition) the lower the density of disintegrated trimers (and/or their life time). Following this logic, the dim C_{60} fullerenes are those molecules which reside atop disintegrated Ag trimers. As the Ag atoms are absent under these fullerenes, they sink deeper by ~1.5 Å (Fig. 3), which is actually an atom scale. In this position, the fullerene adopts a stronger bonding with Si substrate atoms which fixes the molecule in a given orientation, as observed in the experiment (Fig. 2). An additional argument that sounds supportive for the proposed mechanism of dim C_{60} formation stems from the results of calculations in Ref. [35] which show that the most favorable diffusion pathway for Ag adatom on Si(111) $\sqrt{3}\times\sqrt{3}$ – Ag surface is the exchange with Ag adatom constituting the Ag trimer that suggests a possibility for temporal disintegration of Ag trimer.

An indirect confirmation for the proposed origin of dim C_{60} has been gained with the help of ab-initio random structure search (AIRSS) calculations [36,37] where the most principal results are summarized in Fig. 8. In order to simulate the C_{60} monolayer on Si(111) $\sqrt{3}\times\sqrt{3}$ – Ag surface, we have used the supercell models of Si(111) $\sqrt{21}\times\sqrt{21}$ – Ag surface without and with a missing-trimer defect, as shown in Fig. 8a and b, respectively. Three C_{60} molecules adsorb on Si-trimer, small Ag-trimer (or missing-trimer), and large Ag-trimer sites of Si(111) $\sqrt{3}\times\sqrt{3}$ – Ag. The computational details are described in Supplemental material 2 [38]. In the calculations, the most stable adsorption configurations have been evaluated for C_{60} residing atop Ag-trimer (Fig. 8c) and missing-trimer defect (Fig. 8d). One can see that disintegration of small Ag trimer is simulated by expanding Ag–Ag "bond length" from normal 2.85 Å to abnormal 5.44 Å. This rebonding has been found to be characterized by an energy increase of 0.4 eV. However, adsorption energy of C_{60} occupying the missing-trimer defect appears to be 1.1 eV greater than that of C_{60} above small Ag trimer. This result is consistent with the experimental finding that dim C_{60} molecules are in a more tightly bonding state than other molecules. Moreover, it can be treated as supportive for the suggestion that the presence of C_{60} can facilitate (and, at least, justify) disintegration of Ag trimer under the fullerene. Close examination [38] of the bonding configurations reveals that C_{60} adsorption on the small Ag-trimer site disintegrates the average Ag–Ag bond distance from ~3.0 Å to ~8.0 Å and C_{60} in this configuration resides ~1.4 Å lower than C_{60} sitting atop normal small Ag trimer. In the calculations where Ag atoms of the original trimer were removed away from the cell, the height difference was 1.7 and 1.5 Å for C_{60} occupying originally the small and large Ag trimers, respectively. One can see that these evaluations are in good quantitative agreement with the height difference measured with STM (Fig. 3).

With this suggestion, let us consider the origin of tunneling current fluctuations when the fullerene is in the bright C_{60} bonding state. Remind that the measurements were conducted at RT, i.e., above the order–disorder transition. It has been established that at such a temperature the inequivalent triangle (IET) model remains valid, but the surface structure is fluctuating between the two topologically different IET states, so-called IET(+) and IET(−) [33,34]. Thus, if C_{60} resides above an Ag trimer, the latter is changing continuously from large to small Ag trimer and vice versa. Note that C_{60} adsorption energy has to change with these fluctuations (by ~0.17 or ~0.19 eV according to reported [15] and our calculations [38], respectively). Thus, the current fluctuations in Fig. 5 can be attributed to the change in the C_{60} bonding configuration due to transitions between IET(+) and IET(−) states. Estimation of periodicity of fluctuations yields a rate of ~15 Hz. It, however, remains unclear if the presence of C_{60} affects the transition rate between IET(+) and IET(−) or not.

4. Conclusion

In conclusion, we have found that the dark features in the C_{60} arrays on Si(111) $\sqrt{3}\times\sqrt{3}$ – Ag which were interpreted earlier as missing-molecule defects [11] are actually dim C_{60} molecules which are in a more tight bonding configuration and reside ~1.6 Å lower than the other C_{60} molecules. At room temperature, the dynamic switching from bright to dim C_{60} and vice versa takes place. Switching slows down with decreasing temperature and becomes completely frozen at 110 K, which implies that the switching is a thermally driven process. Deposition of ~0.1 monolayer of Ag onto C_{60} array eliminates completely the dim C_{60} molecules. Experimental results can be understood if one assumes that formation of the dim C_{60} is associated with disintegration of Ag trimer on Si(111) $\sqrt{3}\times\sqrt{3}$ – Ag surface under a

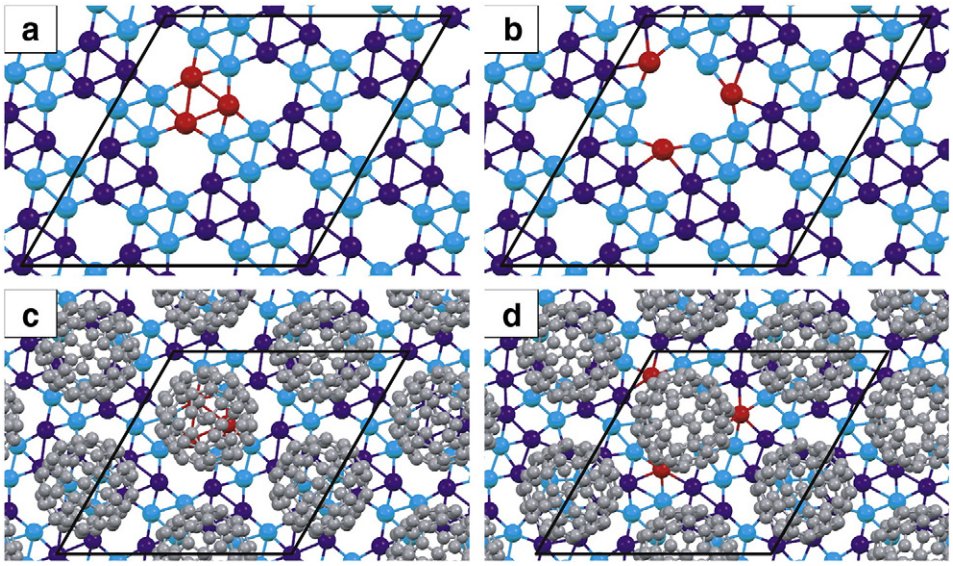

Fig. 8. Structural models of the Si(111) $\sqrt{3} \times \sqrt{3}$ – Ag surface (a) without and (b) with a missing-trimer defect. Only the first surface layer is shown. The most stable configurations of C_{60} monolayer on the surface (c) without and (d) with a missing-trimer defect. The gray, light blue, and deep blue balls are for C, Si, and Ag atoms, respectively. Ag atoms in the position of small Ag-trimer and missing-trimer defect sites are highlighted with red color. The Si(111) $\sqrt{21} \times \sqrt{21}$ super cell is outlined.

given C_{60} fullerene. Results of random structure search calculations support this assumption.

Supplementary data to this article can be found online at http://dx.doi.org/10.1016/j.susc.2013.02.007.

Acknowledgment

Part of this work was supported by the Russian Foundation for Basic Research (grant nos. 11-02-98515, 12-02-00416, 12-02-31832, and 12-02-00430), and the Ministry of Education and Science of the Russian Federation (grant nos. 8022, 8581 and 2.1004.2011) and NSh-774.2012.2.

References

[1] J.A. Gardener, G.A.D. Briggs, M.R. Castell, Phys. Rev. B 80 (2009) 235434.
[2] K. Pussi, H.I. Li, Heekeun Shin, L.N. Serkovic Loli, A.K. Shukla, J. Ledieu, V. Fournée, L.L. Wang, S.Y. Su, K.E. Marino, M.V. Snyder, R.D. Diehl, Phys. Rev. B 86 (2012) 205406.
[3] X.Q. Shi, M.A. Van Hove, R.Q. Zhang, Phys. Rev. B 85 (2012) 075421.
[4] H.I. Li, K. Pussi, K.J. Hanna, L.-L. Wang, D.D. Johnson, H.-P. Cheng, H. Shin, S. Curtarolo, W. Moritz, J.A. Smerdon, R. McGrath, R.D. Diehl, Phys. Rev. Lett. 103 (2009) 056101.
[5] X.Q. Shi, A.B. Pang, K.L. Man, R.Q. Zhang, C. Minot, M.S. Altman, M.A. Van Hove, Phys. Rev. B 84 (2011) 235406.
[6] W.W. Pai, H.T. Jeng, C.-M. Cheng, C.-H. Lin, X. Xiao, A. Zhao, X. Zhang, G. Xu, X.Q. Shi, M.A. Van Hove, C.-S. Hsue, K.-D. Tsuei, Phys. Rev. Lett. 104 (2010) 036103.
[7] L. Tang, X. Zhang, Q. Guo, Y.-N. Wu, L.-L. Wang, H.-P. Cheng, Phys. Rev. B 82 (2010) 125414.
[8] P.J. Moriarty, Surf. Sci. Rep. 65 (2010) 175.
[9] M.D. Upward, P. Moriarty, P.H. Beton, Phys. Rev. B 56 (1997) R1704.
[10] G.L. LeLay, M. Göthelid, V.Y. Aristov, A. Cricenti, M.C. Håkansson, C. Giammichele, P. Perfetti, J. Avila, M.C. Asensio, Surf. Sci. 377/379 (1997) 1061.
[11] T. Nakayama, J. Onoe, K. Takeuchi, M. Aono, Phys. Rev. B 59 (1999) 12627.
[12] K. Tsuchie, T. Nagao, S. Hasegawa, Phys. Rev. B 60 (1999) 11131.
[13] S. Hasegawa, K. Tsuchie, K. Toriyma, X. Tong, T. Nagao, Appl. Surf. Sci. 162 (163) (2000) 42.
[14] M. Nakaya, T. Nakayama, Y. Kuwahara, M. Aono, Surf. Sci. 600 (2006) 2810.
[15] S. Jeong, J. Phys. Soc. Jpn. 79 (2010) 074603.
[16] T. Stimpel, M. Schraufstetter, H. Baumgärtner, I. Eisele, Mater. Sci. Eng. B 89 (2002) 394.
[17] S.H. Chang, I.S. Hwang, C.K. Fang, T.T. Tsong, Phys. Rev. B 77 (2008) 155421.
[18] D.V. Gruznev, A.V. Matetskiy, A.V. Zotov, A.A. Saranin, J.P. Chou, C.M. Wei, Y.L. Wang, Surf. Sci. 605 (2011) 2050.
[19] D.V. Gruznev, A.V. Matetskiy, I.V. Gvozd, A.V. Zotov, A.A. Saranin, Surf. Sci. 605 (2011) 1951.
[20] V.G. Kotlyar, D.A. Olyanich, T.V. Utas, A.V. Zotov, A.A. Saranin, Surf. Sci. 606 (2012) 1821.
[21] A.V. Matetskiy, D.V. Gruznev, A.V. Zotov, A.A. Saranin, Phys. Rev. B 83 (2011) 195421.
[22] See Supplemental Material 1 for STM videos showing dynamic switching between dim and bright C_{60} at various temperatures.
[23] D.A. Tsukanov, M.V. Ryzhkova, E.A. Borisenko, L.V. Bondarenko, A.V. Matetskiy, D.V. Gruznev, A.V. Zotov, A.A. Saranin, J. Appl. Phys. 110 (2011) 093704.
[24] J.N. Crain, M.C. Gallagher, J.L. McChesney, M. Bissen, F.J. Himpsel, Phys. Rev. B 72 (2005) 045312.
[25] C. Liu, I. Matsuda, R. Hobara, S. Hasegawa, Phys. Rev. Lett. 96 (2006) 036803.
[26] H. Jeong, H.W. Yeom, S. Jeong, Phys. Rev. B 77 (2008) 235425.
[27] I. Matsuda, T. Hirahara, M. Konishi, C. Liu, H. Morikawa, M. D'angelo, S. Hasegawa, Phys. Rev. B 71 (2005) 235315.
[28] X. Xie, J.M. Li, W.G. Chen, F. Wang, S.F. Li, Q. Sun, Y. Jia, J. Phys. Condens. Matter 22 (2010) 085001.
[29] I. Matsuda, F. Nakamura, K. Kubo, T. Hirahara, S. Yamazaki, W.H. Choi, H.W. Yeom, H. Narita, Y. Fukuya, M. Hashimoto, A. Kawasuso, M. Ono, Y. Hasegawa, S. Hasegawa, K. Kobayashi, Phys. Rev. B 82 (2010) 165330.
[30] M. D'angelo, M. Konishi, I. Matsuda, C. Liu, S. Hasegawa, T. Okuda, T. Kinoshita, Surf. Sci. 590 (2005) 162.
[31] A.A. Alekseev, V.G. Kotlyar, O.A. Utas, D.V. Gruznev, A.V. Matetskiy, A.V. Zotov, A.A. Saranin, Surf. Sci. 604 (2010) 1400.
[32] H. Tajiri, K. Sumitani, S. Nakatani, A. Nojima, T. Takahashi, K. Akimoto, H. Sugiyama, X. Zhang, H. Kawata, Phys. Rev. B 68 (2003) 035330.
[33] K. Sakamoto, T. Suzuki, K. Mawatari, K. Kobayashi, J. Okabayashi, K. Ono, N. Ueno, M. Oshima, Phys. Rev. B 73 (2006) 193303.
[34] Y. Fukaya, A. Kawasuso, A. Ichimiya, Phys. Rev. B 75 (2007) 115424.
[35] S. Jeong, H. Jeong, Phys. Rev. B 81 (2010) 195429.
[36] C.J. Pickard, R.J. Needs, Phys. Rev. Lett. 97 (2006) 045504.
[37] C.J. Pickard, R.J. Needs, Phys. B Condens. Matter 23 (2011) 053201.
[38] See Supplemental Material 2 for details of AIRSS calculations.